

# An autophagy-related long non-coding RNA signature for glioma

Fangkun Luan<sup>1</sup>, Wenjie Chen<sup>2</sup>, Miao Chen<sup>1</sup>, Jun Yan<sup>1</sup>, Hao Chen<sup>1</sup>, Haiyue Yu<sup>1</sup>, Tieqi Liu<sup>1</sup> and Ligen Mo<sup>1</sup>

<sup>1</sup> Department of Neurosurgery, Affiliated Tumor Hospital of Guangxi Medical University, Nanning, China

<sup>2</sup> Department of Ultrasound, Affiliated Tumor Hospital of Guangxi Medical University, Nanning, China

## Keywords

autophagy; CCGA; glioma; long non-coding RNA; prognostic signature; TCGA

## Correspondence

L. Mo, Department of Neurosurgery, Affiliated Tumor Hospital of Guangxi Medical University, Nanning, Guangxi Zhuang Autonomous Region 530021, China  
Fax: +86 0771 5312000  
Tel: +86 0771 5302321  
E-mail: ligenmo@163.com

Fangkun Luan and Wenjie Chen contributed equally to this article

(Received 14 September 2018, revised 30 November 2018, accepted 21 January 2019)

doi:10.1002/2211-5463.12601

Glioma is one of the most common types of malignant primary central nervous system tumor, and prognosis for this disease is poor. As autophagic drugs have been reported to induce glioma cell death, we investigated the potential prognostic role of autophagy-associated long non-coding RNA (lncRNA) in glioma patients. In this study, we obtained 879 lncRNAs and 216 autophagy genes from the Chinese Glioma Genome Atlas microarray, and found that 402 lncRNAs are correlated with the autophagy genes. Subsequently, 10 autophagy-associated lncRNAs with prognostic value (*PCBP1-AS1*, *TP53TG1*, *DHRS4-AS1*, *ZNF674-AS1*, *GABPB1-AS1*, *DDX11-AS1*, *SBF2-AS1*, *MIR4453HG*, *MAPKAPK5-AS1* and *COX10-AS1*) were identified in glioma patients using multivariate Cox regression analyses. A prognostic signature was then established based on these prognostic lncRNAs, dividing patients into low-risk and high-risk groups. The overall survival time was shorter in the high-risk group than that in the low-risk group [hazard ratio (HR) = 5.307, 95% CI: 4.195–8.305;  $P < 0.0001$ ]. Gene set enrichment analysis revealed that the gene sets were significantly enriched in cancer-related pathways, including interleukin (IL) 6/Janus kinase/signal transducer and activator of transcription (STAT) 3 signaling, tumor necrosis factor  $\alpha$  signaling via nuclear factor  $\kappa$ B, IL2/STAT5 signaling, the p53 pathway and the KRAS signaling pathway. The Cancer Genome Atlas dataset was used to validate that high-risk patients have worse survival outcomes than low-risk patients (HR = 1.544, 95% CI: 1.110–2.231;  $P = 0.031$ ). In summary, our signature of 10 autophagy-related lncRNAs has prognostic potential for glioma, and these autophagy-related lncRNAs may play a key role in glioma biology.

Glioma is one of the most common types of malignant primary central nervous system tumors with poor prognosis, comprising approximately 44% of central nervous system tumors [1]. The prognosis of glioblastoma (GBM) is the worst among gliomas, in

which the median overall survival (OS) for patients with GBM is 15–23 months and the 5-year survival rate is less than 6% [2,3]. Upon diagnosis, the standard treatment of glioma includes maximal surgical resection, chemotherapy, such as temozolomide, and

## Abbreviations

CGGA, Chinese Glioma Genome Atlas; GBM, glioblastoma; GSEA, gene set enrichment analysis; HCC, hepatocellular carcinoma; *HOTAIR*, *HOX* (homeobox) transcript antisense RNA; HR, hazard ratio; IFN, interferon; IL, interleukin; lncRNA, long non-coding RNA; miRNA, microRNA; MMP, matrix metalloproteinase; OS, overall survival; STAT, signal transducer and activator of transcription; TCGA, The Cancer Genome Atlas.

**Table 1.** Correlation between the prognostic lncRNAs and autophagy genes in glioma.

lncRNA	Autophagy gene	Correlation	P
PCBP1-AS1	CCL2	-0.360049202	2.2072E-11
PCBP1-AS1	ATG2B	0.304817007	2.0467E-08
PCBP1-AS1	KIF5B	0.305876376	1.818E-08
PCBP1-AS1	ATG2A	0.311692494	9.4056E-09
PCBP1-AS1	WDFY3	0.31817447	4.4365E-09
PCBP1-AS1	MLST8	0.322140176	2.7765E-09
PCBP1-AS1	PIK3C3	0.324642153	2.0586E-09
PCBP1-AS1	TSC1	0.330291284	3.8213E-09
PCBP1-AS1	TSC2	0.332514623	8.3751E-10
PCBP1-AS1	NCKAP1	0.339888292	3.3348E-10
PCBP1-AS1	GRID2	0.364527555	5.5069E-11
PCBP1-AS1	SIRT2	0.366890173	8.5922E-12
PCBP1-AS1	MTOR	0.371080649	4.7675E-12
PCBP1-AS1	SIRT1	0.385311738	6.0485E-13
PCBP1-AS1	NBR1	0.3900753	3.5039E-13
PCBP1-AS1	ERBB2	0.398520286	8.1268E-14
PCBP1-AS1	BIRC6	0.401737956	4.9072E-14
PCBP1-AS1	HDAC6	0.410137987	1.2879E-14
PCBP1-AS1	KIAA0226	0.417146773	3.9968E-15
PCBP1-AS1	RPTOR	0.426641207	8.8818E-16
TP53TG1	GABARAP	0.44046552	0
TP53TG1	TM9SF1	0.440120961	0
TP53TG1	VAMP3	0.43087095	4.4409E-16
TP53TG1	ITGB4	0.379361437	1.4515E-12
TP53TG1	LAMP1	0.362507507	1.5766E-11
TP53TG1	RHEB	0.338549143	3.7103E-10
TP53TG1	FADD	0.322540605	2.6472E-09
TP53TG1	RAB7A	0.320497198	3.3743E-09
TP53TG1	HDAC1	0.316709215	5.2662E-09
TP53TG1	ATG4B	0.310888419	1.0312E-08
TP53TG1	DIRAS3	0.305503826	1.8954E-08
TP53TG1	RGS19	0.300279741	3.5506E-08
DHRS4-AS1	PRKAR1A	0.304280356	2.6545E-08
DHRS4-AS1	BIRC6	0.307830991	1.7911E-08
DHRS4-AS1	RPTOR	0.313316207	9.6535E-09
DHRS4-AS1	WDFY3	0.314945434	8.0148E-09
DHRS4-AS1	GOPC	0.319627801	5.2128E-09
DHRS4-AS1	MAPK1	0.320002607	4.4667E-09
DHRS4-AS1	ST13	0.322382713	3.3795E-09
DHRS4-AS1	PIK3R4	0.323543353	2.9471E-09
DHRS4-AS1	NCKAP1	0.367547056	1.0542E-11
DHRS4-AS1	SIRT1	0.40099047	7.8826E-14
DHRS4-AS1	NBR1	0.430691637	6.6613E-16
ZNF674-AS1	ITPR1	-0.319258764	1.3176E-08
ZNF674-AS1	TP53INP2	-0.313961307	7.2452E-09
ZNF674-AS1	EIF2S1	0.304321171	2.163E-08
ZNF674-AS1	PARP1	0.311082339	1.0086E-08
ZNF674-AS1	HDAC1	0.311370172	9.7591E-09
ZNF674-AS1	EEF2K	0.319838206	3.6476E-09
ZNF674-AS1	TM9SF1	0.321374147	3.0412E-09
ZNF674-AS1	GNAI3	0.331509862	8.9278E-10
ZNF674-AS1	FKBP1A	0.339350907	3.3524E-10
ZNF674-AS1	ATG4B	0.34228221	2.308E-10

**Table 1.** (Continued).

lncRNA	Autophagy gene	Correlation	P
ZNF674-AS1	PELP1	0.342564645	2.226E-10
ZNF674-AS1	FADD	0.344531987	1.7285E-10
ZNF674-AS1	ENSG00000177993.3	0.344786314	1.6727E-10
ZNF674-AS1	HGS	0.349662833	8.8614E-11
ZNF674-AS1	WDR45	0.350583974	7.8496E-11
ZNF674-AS1	CAPN10	0.357666059	3.0499E-11
ZNF674-AS1	RHEB	0.357722928	3.0266E-11
ZNF674-AS1	MAP1LC3C	0.358011106	2.9109E-11
ZNF674-AS1	BIRC5	0.365800568	3.2339E-11
ZNF674-AS1	MAP2K7	0.37311006	3.5731E-12
ZNF674-AS1	STK11	0.375183168	2.6561E-12
ZNF674-AS1	GNB2L1	0.402865027	4.1078E-14
ZNF674-AS1	PRKAB1	0.411848633	9.77E-15
ZNF674-AS1	EIF4EBP1	0.441387008	0
ZNF674-AS1	RAF1	0.471527103	0
ZNF674-AS1	HDAC6	0.529212582	0
MAPKAPK5-AS1	DLC1	-0.37599408	2.7613E-12
MAPKAPK5-AS1	CTSB	-0.321021809	3.1711E-09
MAPKAPK5-AS1	RGS19	-0.304801176	2.1559E-08
MAPKAPK5-AS1	PRKCD	-0.303327412	7.978E-08
MAPKAPK5-AS1	APOL1	-0.301552957	5.851E-08
MAPKAPK5-AS1	EIF2S1	0.306873043	1.6255E-08
MAPKAPK5-AS1	STK11	0.316360528	5.4847E-09
MAPKAPK5-AS1	ATG3	0.317029326	5.073E-09
MAPKAPK5-AS1	GNB2L1	0.325707112	1.8109E-09
MAPKAPK5-AS1	PRKAB1	0.332894214	7.5251E-10
MAPKAPK5-AS1	MAP2K7	0.334240467	6.3674E-10
MAPKAPK5-AS1	ATG4B	0.342782716	2.1647E-10
MAPKAPK5-AS1	GABARAPL2	0.344580777	1.7176E-10
MAPKAPK5-AS1	RAF1	0.368047755	7.3084E-12
MAPKAPK5-AS1	HDAC6	0.370823221	4.9445E-12
MAPKAPK5-AS1	HGS	0.373857161	3.2117E-12
MAPKAPK5-AS1	BID	0.396105786	1.1813E-13
MAPKAPK5-AS1	RAB24	0.404333356	3.2641E-14
MAPKAPK5-AS1	GABARAP	0.420904922	2.2204E-15
MAPKAPK5-AS1	PELP1	0.451556383	0
MAPKAPK5-AS1	CDKN1B	0.456366201	0
COX10-AS1	MAP1LC3A	-0.375521773	2.53E-12
COX10-AS1	TP53INP2	-0.369627107	5.854E-12
COX10-AS1	PINK1	-0.367447805	7.9483E-12
COX10-AS1	GABARAPL1	-0.345745019	1.4775E-10
COX10-AS1	HDAC1	0.30053166	3.2895E-08
COX10-AS1	FKBP1A	0.305650956	1.8644E-08
COX10-AS1	RB1	0.307329731	1.544E-08
COX10-AS1	ATF6	0.308265668	1.3892E-08
COX10-AS1	HGS	0.312518629	8.5551E-09
COX10-AS1	NAF1	0.313398471	7.7313E-09
COX10-AS1	PIK3C3	0.323065939	2.4864E-09
COX10-AS1	ITGB1	0.330112011	1.0601E-09
COX10-AS1	PRKAB1	0.333014795	7.4136E-10
COX10-AS1	GNB2L1	0.344926977	1.6425E-10
COX10-AS1	PARP1	0.345318807	1.5614E-10
COX10-AS1	EIF2S1	0.3460972	1.4116E-10

Table 1. (Continued).

lncRNA	Autophagy gene	Correlation	P
COX10-AS1	FADD	0.361593998	1.7871E-11
COX10-AS1	MYC	0.375188431	2.6541E-12
COX10-AS1	EEF2K	0.377661311	1.8581E-12
COX10-AS1	EIF4EBP1	0.405855635	2.5757E-14
COX10-AS1	EIF2AK3	0.419195952	2.8866E-15
COX10-AS1	HDAC6	0.428787718	4.4409E-16
COX10-AS1	GNAI3	0.439816001	0
COX10-AS1	BIRC5	0.448936102	0
COX10-AS1	RAF1	0.572860513	0
GABPB1-AS1	BID	0.420118584	2.4425E-15
GABPB1-AS1	BIRC6	0.36038314	2.1089E-11
GABPB1-AS1	CASP4	-0.343935388	5.2362E-10
GABPB1-AS1	CCL2	-0.373849011	3.2156E-12
GABPB1-AS1	CCR2	-0.368177579	3.6858E-11
GABPB1-AS1	CDKN1B	0.364553409	1.1889E-11
GABPB1-AS1	CTSB	-0.372819935	3.7241E-12
GABPB1-AS1	CTSD	-0.43970168	0
GABPB1-AS1	DAPK1	0.323366578	2.3986E-09
GABPB1-AS1	DIRAS3	-0.300618621	3.2582E-08
GABPB1-AS1	DLC1	-0.313694777	8.3115E-09
GABPB1-AS1	DNAJB1	-0.308644775	1.3309E-08
GABPB1-AS1	EEF2	0.36428838	1.2333E-11
GABPB1-AS1	GNB2L1	0.304868539	2.0349E-08
GABPB1-AS1	GRID2	0.358164661	1.2447E-10
GABPB1-AS1	HDAC6	0.583737387	0
GABPB1-AS1	KLHL24	0.37211066	4.1194E-12
GABPB1-AS1	MAP1LC3A	-0.335686931	5.3165E-10
GABPB1-AS1	MAP2K7	0.351129758	7.3042E-11
GABPB1-AS1	MYC	0.350474546	7.9636E-11
GABPB1-AS1	NAMPT	-0.317006934	5.0863E-09
GABPB1-AS1	PARP1	0.318853967	4.0962E-09
GABPB1-AS1	PEA15	0.306793364	1.6401E-08
GABPB1-AS1	PELP1	0.350174812	8.2843E-11
GABPB1-AS1	PPP1R15A	-0.432497553	4.4409E-16
GABPB1-AS1	PRKCD	-0.354522637	2.4201E-10
GABPB1-AS1	RAF1	0.518711717	0
GABPB1-AS1	SERPINA1	-0.35246404	9.1958E-11
GABPB1-AS1	SIRT1	0.377399334	1.9298E-12
GABPB1-AS1	SQSTM1	-0.300514253	3.2958E-08
GABPB1-AS1	VAMP3	-0.349193236	9.4249E-11
GABPB1-AS1	WIPI1	-0.425794454	8.8818E-16
DDX11-AS1	PINK1	-0.380737586	1.1873E-12
DDX11-AS1	PRKCD	-0.337496704	1.8761E-09
DDX11-AS1	MAP1LC3A	-0.321966423	2.8346E-09
DDX11-AS1	TP53INP2	-0.315547251	6.0291E-09
DDX11-AS1	EIF2AK3	0.301487968	2.9609E-08
DDX11-AS1	EIF2S1	0.34484361	1.6603E-10
DDX11-AS1	FKBP1A	0.36028176	2.1383E-11
DDX11-AS1	MAP2K7	0.361662635	1.7704E-11
DDX11-AS1	MYC	0.36701736	8.4412E-12
DDX11-AS1	PRKAB1	0.367277985	8.1393E-12
DDX11-AS1	HGS	0.398721365	7.8604E-14
DDX11-AS1	PARP1	0.399014394	7.5051E-14
DDX11-AS1	GNB2L1	0.446121011	0
DDX11-AS1	HDAC6	0.4630659	0

Table 1. (Continued).

lncRNA	Autophagy gene	Correlation	P
DDX11-AS1	BIRC5	0.494242839	0
DDX11-AS1	EIF4EBP1	0.494327951	0
DDX11-AS1	RAF1	0.595959165	0
SBF2-AS1	SIRT1	-0.359724478	2.6578E-11
SBF2-AS1	BID	-0.359318057	2.8079E-11
SBF2-AS1	EEF2	-0.345315983	1.7787E-10
SBF2-AS1	HDAC6	-0.30180643	3.1545E-08
SBF2-AS1	HSPA5	0.303106799	2.7341E-08
SBF2-AS1	NAMPT	0.305876474	2.0115E-08
SBF2-AS1	DLC1	0.313900704	9.0314E-09
SBF2-AS1	PPP1R15A	0.315700878	6.5975E-09
SBF2-AS1	FKBP1B	0.330524677	1.1347E-09
SBF2-AS1	WIPI1	0.347602864	1.3239E-10
SBF2-AS1	DIRAS3	0.34895202	1.111E-10
SBF2-AS1	CFLAR	0.353930283	5.7749E-11
SBF2-AS1	CCR2	0.365426608	6.1051E-11
SBF2-AS1	CASP4	0.387535164	1.7764E-12
SBF2-AS1	CTSD	0.39811287	1.0303E-13
SBF2-AS1	RAB33B	0.41262521	1.0436E-14
SBF2-AS1	MAP1LC3A	0.466078431	0
MIR4453HG	BIRC6	0.482298774	0
MIR4453HG	CCL2	-0.32967133	1.1188E-09
MIR4453HG	CCR2	-0.306263916	5.3174E-08
MIR4453HG	CDKN1B	0.37854434	1.6347E-12
MIR4453HG	CTSD	-0.36405224	1.2743E-11
MIR4453HG	EEF2	0.339277778	3.3836E-10
MIR4453HG	EIF2AK3	0.30731381	1.5468E-08
MIR4453HG	EIF2S1	0.300378118	3.3454E-08
MIR4453HG	ERBB2	0.31509245	6.356E-09
MIR4453HG	GRID2	0.33900455	1.3033E-09
MIR4453HG	HDAC6	0.530273615	0
MIR4453HG	MBTPS2	0.372080137	4.1376E-12
MIR4453HG	MLST8	0.336179553	4.9987E-10
MIR4453HG	NAF1	0.343120261	2.0729E-10
MIR4453HG	NBR1	0.332149604	9.3012E-10
MIR4453HG	NCKAP1	0.315032585	6.7536E-09
MIR4453HG	PIK3C3	0.398066735	8.7041E-14
MIR4453HG	PIK3R4	0.383400705	8.0247E-13
MIR4453HG	RAF1	0.446543819	0
MIR4453HG	SERPINA1	-0.316157599	7.7713E-09
MIR4453HG	SIRT1	0.394985589	1.4033E-13
MIR4453HG	ST13	0.343209924	2.0492E-10
MIR4453HG	TSC2	0.324952539	2.1001E-09
MIR4453HG	USP10	0.330643906	1.3364E-09
MIR4453HG	VAMP3	-0.34420749	1.8024E-10
MIR4453HG	WDFY3	0.321627435	2.9511E-09
MIR4453HG	WIPI1	-0.324415393	2.1154E-09

radiation. Treatment options may vary in different stages of the disease and by the age of the patients. Various factors affect the prognosis of GBM including *EGFR* amplifications, and mutations of *IDH1*, *TP53* and *PTEN* [4–6]. However, the survival

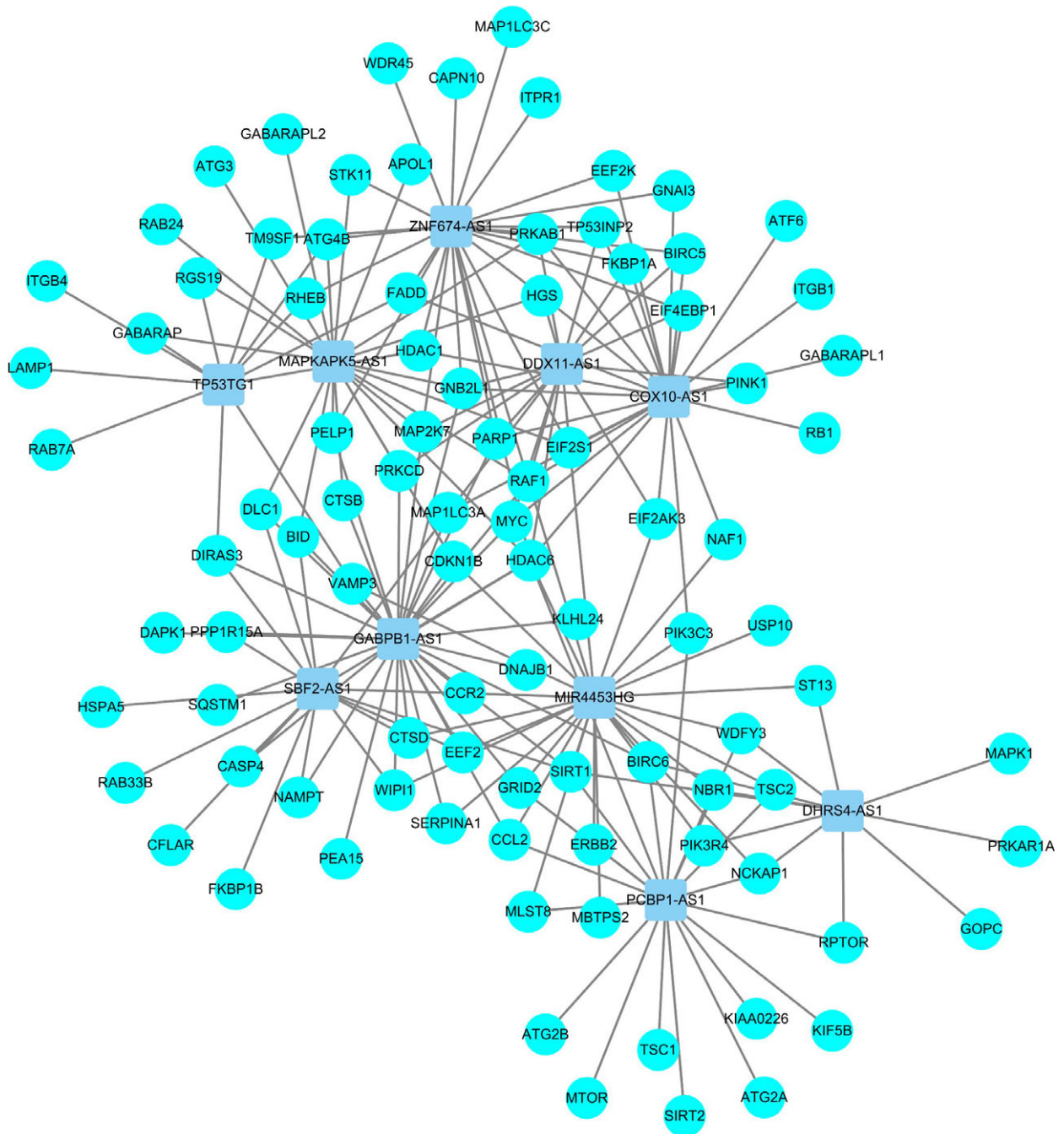


**Fig. 1.** Network of prognostic lncRNAs with co-expressed autophagy genes in glioma. In the centric position, grey blue nodes indicate lncRNAs and the sky blue indicates autophagy genes. The coexpression network is visualized by Cytoscape 3.4 software.

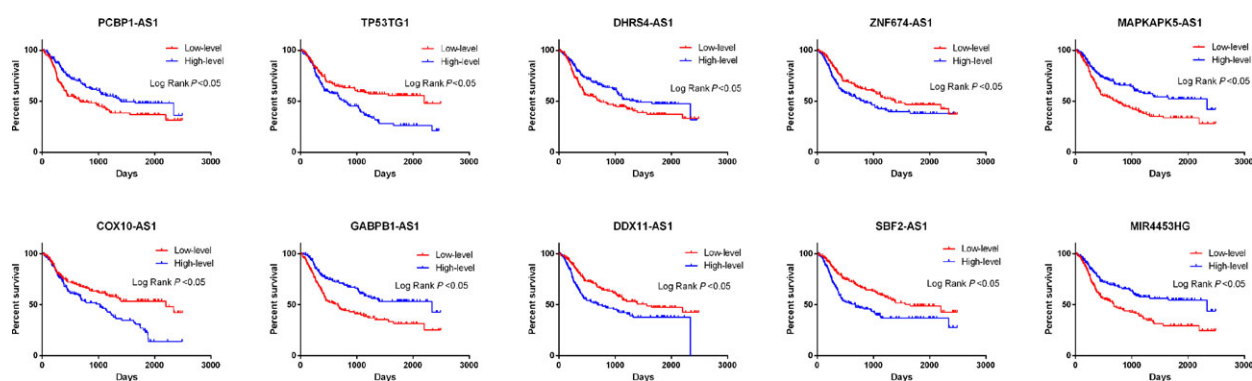
outcome is unfavorable due to the complex genetic mechanism.

Autophagy is the physiological process that directs degradation of proteins and whole organelles in cells. The activation of autophagy is divided into normal and pathological conditions. Under normal

circumstances, autophagy represents a response to several stresses by providing the necessary circulating metabolic substrates for survival. In addition, autophagy is active in some pathological processes in order to maintain cellular homeostasis, such as neurodegenerative diseases, pathogenic inflammation,

**Table 2.** Detailed information for 10 autophagy-related lncRNAs significantly associated with OS in glioma.

lncRNA	Ensemble ID	$\beta$	SE	<i>P</i>	HR	Lower	Upper
<i>PCBP1-AS1</i>	ENSG00000179818	-0.363	0.184	0.049	0.696	0.485	0.998
<i>TP53TG1</i>	ENSG00000182165	0.443	0.16	0.006	1.558	1.139	2.131
<i>DHRS4-AS1</i>	ENSG00000215256	-0.253	0.099	0.01	0.776	0.639	0.942
<i>ZNF674-AS1</i>	ENSG00000230844	0.448	0.199	0.024	1.565	1.06	2.31
<i>MAPKAPK5-AS1</i>	ENSG00000234608	-0.64	0.245	0.009	0.527	0.326	0.852
<i>COX10-AS1</i>	ENSG00000236088	0.829	0.194	< 0.001	2.29	1.565	3.351
<i>GABPB1-AS1</i>	ENSG00000244879	-0.403	0.154	0.009	0.668	0.494	0.904
<i>DDX11-AS1</i>	ENSG00000245614	0.296	0.128	0.021	1.344	1.046	1.726
<i>SBF2-AS1</i>	ENSG00000246273	0.134	0.064	0.036	1.143	1.009	1.295
<i>MIR4453HG</i>	ENSG00000268471	-0.551	0.155	< 0.001	0.577	0.426	0.781

**Fig. 2.** Kaplan–Meier survival curves for the 10 prognostic lncRNAs for glioma in CCGA dataset. The 10 autophagy-related lncRNAs were found to be independent prognostic factors for glioma patients, of which five lncRNAs were unfavorable factors (*TP53TG1*, *ZNF674-AS1*, *COX10-AS1*, *DDX11-AS1* and *SBF2-AS1*) and five lncRNAs were confirmed to be favorable prognostic factors for glioma (*PCBP1-AS1*, *DHRS4-AS1*, *GABPB1-AS1*, *MAPKAPK5-AS1* and *MIR4453HG*).

aging and cancer [7]. In recent years, many studies have sought to find new potential targeted therapies by investigating autophagy pathways [8–10]. In addition, autophagic drugs induce cell autophagic death (type II cell death) and cause glioma cell death. Whether this is an alternative and emerging concept for the study of novel glioma therapies remains largely unknown [11].

Long non-coding RNAs (lncRNAs) have a wide range of functional activities [12]. They play a significant role in physiological processes, including RNA decay, genetic regulation of gene expression, RNA splicing, microRNA (miRNA) regulation and protein folding [13]. lncRNA regulates many proteins that are important for autophagy. Impaired functioning of lncRNAs participates in glioma pathogenesis, such as cellular apoptosis and proliferation [14]. *HOX* (homeobox) transcript antisense RNA (*HOTAIR*) is a lncRNA that plays an important role in the

regulation of cancer transformation, mainly due to extensive miRNA–*HOTAIR* interactions and its effect on matrix metalloproteinases (MMPs) [15]. There may be an involvement of *HOTAIR*-interacting miRNAs and MMPs in autophagy regulation [16–18]. Sufficient evidence shows that lncRNAs mediate transcriptional and post-transcriptional levels of autophagy-related genes to regulate the autophagy regulatory network [19,20]. This paper proposes to construct a coexpression network of autophagy-related lncRNAs using bioinformatics methods, providing a theoretical basis for the treatment of gliomas [21].

Therefore, autophagy-related lncRNAs may have potential value in the prognosis of glioma patients and may serve as potential therapeutic targets. Here, we aimed to establish an autophagy-related lncRNA signature in glioma and to advance the targeted treatment of glioma.

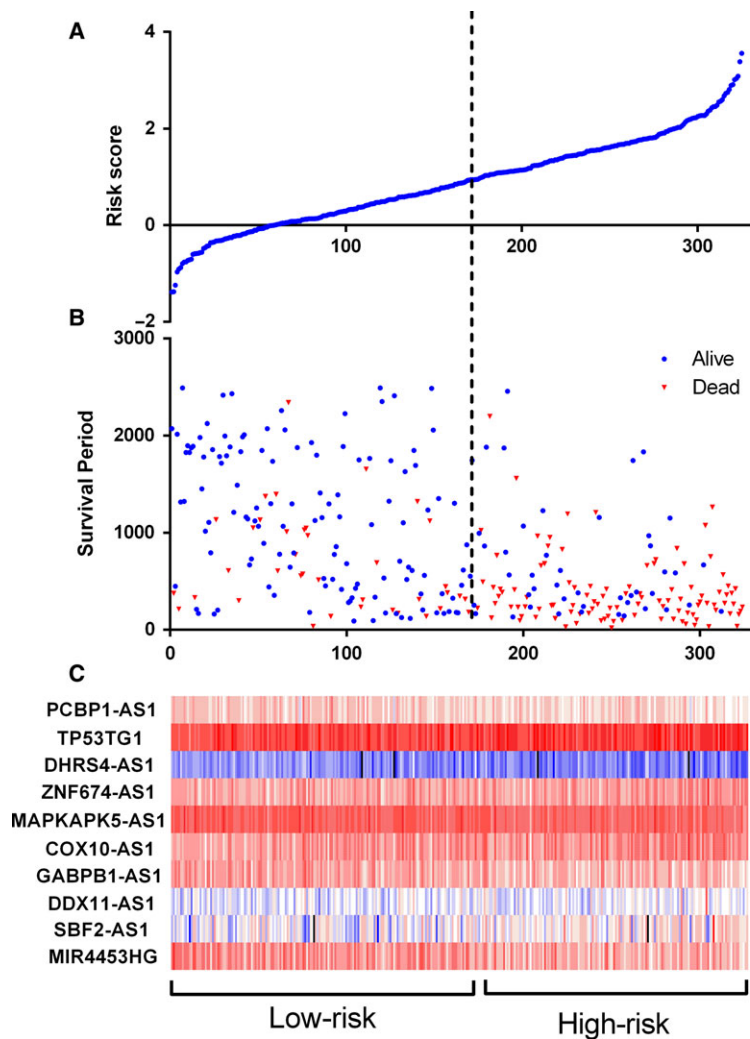


**Fig. 3.** Autophagy-related lncRNA risk score analysis of glioma patients in CCGA. (A) The low and high score group for the autophagy-related lncRNA signature in glioma patients. (B) The survival status and duration of glioma cases. (C) Heatmap of the 10 key lncRNAs expression in glioma. The color from blue to red shows an increasing trend from low levels to high levels.

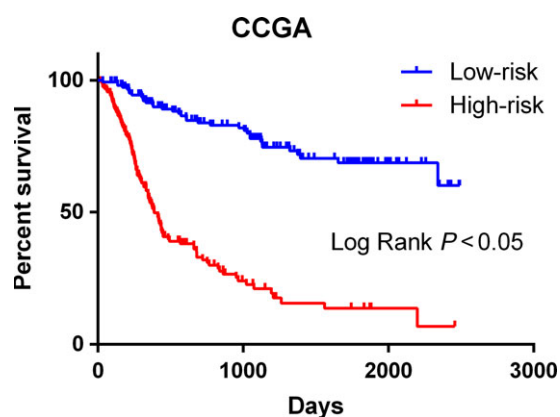


**Fig. 4.** Kaplan–Meier survival curves for the autophagy-related lncRNA risk score for glioma in CCGA dataset. The Kaplan–Meier survival curves showed that the OS period is longer in the low-risk group than that in the high-risk group in the CCGA datasets (median OS 1211 vs 346 days; log rank  $P < 0.05$ ).

## Materials and methods

### Information extraction of glioma patients

The Chinese Glioma Genome Atlas (CGGA, <http://www.cgga.org.cn/>, freely available) microarray was used as a training set to establish an autophagy-associated lncRNA signature of glioma patients. CGGA is the largest glioma tissue database with follow-ups in China. Thousands of samples have been subjected to whole-exome sequencing, DNA methylation microarray detection and whole-genome sequencing, miRNA, mRNA and circRNA sequencing. The training dataset includes CGGA mRNA expression (FPKM) in 325 glioma patients together with relevant clinical data. The patients were diagnosed based on the 2007 WHO classification guidelines. We downloaded clinical information from the dataset website. The prognostic signature was further validated based on The Cancer Genome Atlas (TCGA, <https://cancergenome.nih.gov/>) GBM

**Table 3.** Multivariate Cox regression analysis of characteristics and risk score in glioma.

Variable	$\beta$	SE	Wald	<i>P</i>	HR	Lower	Upper
Gender	-0.022	0.221	0.01	0.921	0.978	0.635	1.507
Age	0	0.01	0	0.987	1	0.98	1.021
Grade	0.831	0.16	26.965	< 0.001	2.296	1.678	3.143
Radiotherapy	-0.932	0.206	20.553	< 0.001	0.394	0.263	0.589
Chemotherapy	-0.469	0.207	5.143	0.023	0.626	0.417	0.938
<i>IDHDampR</i>	-0.639	0.248	6.641	0.01	0.528	0.324	0.858
<i>TP53.1</i>	-0.334	0.186	3.23	0.072	0.716	0.498	1.031
<i>EGFR</i>	-0.165	0.212	0.605	0.437	0.848	0.559	1.285
<i>ATRX</i>	-0.817	0.41	3.98	0.046	0.442	0.198	0.986
<i>EZH2</i>	0.477	0.271	3.104	0.078	1.612	0.948	2.742
Risk score	1.006	0.243	17.156	< 0.001	2.736	1.699	4.405

**Table 4.** Clinical impact of risk score signature for the CCGA cohort.

Clinicopathological feature	<i>n</i>	Risk score		<i>t</i>	<i>P</i>
		Mean	SD		
Grade					
I-II	216	1.203847424	0.8808	10.898	< 0.001
III-IV	109	0.245607385	0.6717		
Radiotherapy					
Yes	212	0.777059137	0.9674	-2.267	0.025
No	84	1.029456602	0.8189		
Chemotherapy					
Yes	158	1.01284085	0.8665	2.604	0.01
No	128	0.727299406	0.9862		
IDH (DNA and RNA)					
Mutation	171	0.497626264	0.8174	-8.69	< 0.001
Wildtype	154	1.30979323	0.8671		
IDH1-R32					
Wildtype	162	0.509472199	0.8242	-7.824	< 0.001
Mutation	163	1.253176395	0.8881		
<i>TP53.1</i>					
Wildtype	189	0.937494898	0.9505	1.254	0.211
Mutation	136	0.805997888	0.9062		
<i>EGFR</i>					
Wildtype	110	0.770831973	0.9802	-1.546	0.123
Mutation	215	0.939584798	0.905		
<i>ATRX</i>					
Wildtype	33	0.856142312	0.9358	-0.171	0.865
Mutation	292	0.885443672	0.9343		
<i>EZH2</i>					
Wildtype	37	1.182088779	1.1162	1.77	0.084
Mutation	288	0.843975569	0.9019		

dataset. TCGA GBM dataset (FPKM level 3) was included in our analysis as a validation dataset with 160 GBM patients.

### lncRNA and autophagy gene screening

The profiles of lncRNAs and autophagy genes were obtained from the CGGA ALL mRNAseq dataset.

Specifically, the autophagy gene list was obtained from the Human Autophagy Database (HADb, <http://autophagy.lu/clustering/index.html>). All of the mRNA expression data were normalized by log<sub>2</sub> transformation. Pearson correlation was applied to calculate the correlation between the lncRNAs and autophagy-related genes. A lncRNA with a correlation coefficient  $|R^2| > 0.3$  and  $P < 0.05$  was considered to be an autophagy-related lncRNA.

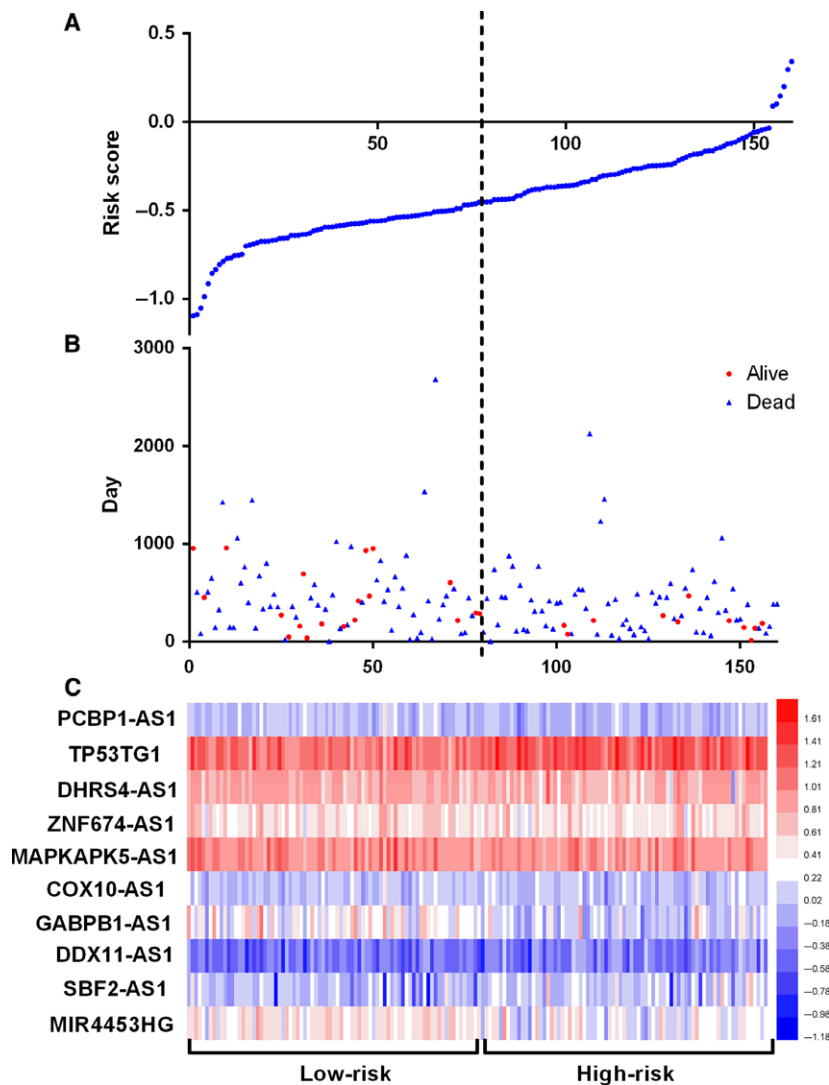


**Fig. 5.** Autophagy-related lncRNA risk score analysis of glioma patients in TCGA. (A) The low and high score group for the autophagy-related lncRNA signature in glioma patients. (B) The survival status and duration of glioma cases. (C) Heatmap of the 10 key lncRNAs expressed in glioma. The color from blue to red shows an increasing trend from low levels to high levels.

### Signature development

First, univariate and multivariate Cox regression analyses were performed to evaluate the prognostic value of autophagy-related lncRNAs. The lncRNAs with a  $P$ -value  $< 0.01$  by univariate analysis were included in the multivariate stepwise regression Cox analysis to establish the risk score. We used the previous report to determine the risk score for each patient using the following formula: Risk score =  $\beta_{\text{gene1}} \times \text{expr}_{\text{gene1}} + \beta_{\text{gene2}} \times \text{expr}_{\text{gene2}} + \dots + \beta_{\text{genen}} \times \text{expr}_{\text{genen}}$ . Cox analysis was performed to build a signature for predicting survival. For more detail, we assigned risk scores by a linear combination of the expression levels of lncRNAs weighted by regression coefficients ( $\beta$ ). The  $\beta$  value was calculated by log transformation of the hazard ratio (HR) from the multivariate Cox regression analysis. High-risk and low-risk groups were established based on the median risk score. The lncRNA expression is defined as  $\text{expr}_{\text{genen}}$ .

### Gene set enrichment analysis

Gene set enrichment analysis (GSEA) was used to interpret gene expression data. This method derives its function by analyzing gene sets, so it can be used to determine whether the gene set shows a statistically significant difference between the two biological states. In this study, we verified whether genes that are differentially expressed between two groups are enriched during autophagy.

### Statistical analysis

The expression levels of autophagy-related lncRNAs were elevated ( $P \leq 0.05$ ). Construction of the autophagy-lncRNA coexpression network was completed using CYTOSCAPE software [22] (version 3.4.0; The Cytoscape Consortium, San Diego, CA, USA). Pearson correlation analysis and Cox regression analysis were performed using SPSS STATISTICS software (version 24; IBM Corp., Armonk,



NY, USA). Survival status was the basis for univariate cox regression analysis. PRISM 7 (GraphPad Software Inc., La Jolla, CA, USA) was used to generate Kaplan–Meier curves. GSEA (<http://www.broadinstitute.org/gsea/index.jsp>) was used to distinguish between two sets of functional annotations. Statistical significance was set at a threshold of a two-tailed  $P < 0.05$ .

## Results

### Construction of a coexpression network for autophagy–lncRNAs

We identified a total of 878 lncRNAs in the CGGA dataset, which was extracted from the CGGA database. A total of 215 autophagy-related genes were extracted from the Human Autophagy Database (HADb, <http://autophagy.lu/clustering/index.html>). We constructed an autophagy–lncRNA coexpression network to identify autophagy-related lncRNAs. Finally, 402 lncRNAs were identified ( $|R^2| > 0.3$  and  $P \leq 0.05$ ).

### Identification of a signature of 10 autophagy-related lncRNAs in patients with glioma

First, we identified autophagy-related lncRNAs by constructing autophagy–lncRNA coexpression networks ( $P \leq 0.05$ ). In addition, we used univariate Cox regression analysis based on 402 autophagy-associated lncRNAs to screen prognostic genes. We ranked the prognostic autophagy-related lncRNAs in ascending order by their  $P$  values. We used a  $P$  value of 0.05 as the cutoff value, and the lncRNAs that satisfied this were used for signature development. Our training set was a collection of 325 glioma patients from the CGGA dataset. A total of 19 lncRNAs have prognostic value for glioma patients ( $P < 0.01$ ). Subsequently, 10 autophagy-related lncRNAs were found to be independent prognostic factors for glioma patients (Table 1 and Fig. 1), of which five lncRNAs were unfavorable factors (*TP53TG1*, *ZNF674-AS1*, *COX10-AS1*, *DDX11-AS1* and *SBF2-AS1*) and five lncRNAs were confirmed to be favorable prognostic factors for glioma (*PCBP1-AS1*, *DHRS4-AS1*, *GABPB1-AS1*, *MAPKAPK5-AS1* and *MIR4453HG*) (Table 2 and Fig. 2).

### The prognostic impact of an autophagy-related lncRNA signature for glioma

Next, we use a risk score method to develop an autophagy-related lncRNA signature. We divided the glioma patients into two groups (low-risk group and high-risk

group) by median risk score (Fig. 3). As a result, the risk score could significantly predict the OS of glioma patients, in which the OS period is longer in the low-risk group than that in the high-risk group (median OS 1211 vs 346 days; log rank  $P < 0.05$ ). Additionally, the Cox regression analysis also revealed a significant prognostic effect of the risk score on the glioma patients (HR = 5.307, 95% CI: 4.195–8.305;  $P < 0.0001$ , Fig. 4). Further, we also explored whether the risk score signature is an independent predictor for the prognosis of glioma patients by multivariate Cox regression analysis. As a consequence, a HR of 2.736 indicated that the risk score could significantly contribute to the prediction of survival of glioma patients, eliminating the influence of other factors such as sex, age, grade, radiotherapy, chemotherapy and the molecular status (*IDHDampR*, *TP53.1*, *EGFR*, *ATRX* and *EZH2*) (Table 3).

### Clinical value of the lncRNA signature for glioma patients

Subsequently, we also determined the clinical value of the 10-lncRNA signature regarding the grade, radiotherapy and chemotherapy. As shown in the Table 4, the risk score tends to increase in the higher grades, suggesting that this lncRNA signature might be associated with the progression of glioma. Interestingly, the risk score was lower in patients receiving radiotherapy than that in patients without radiotherapy ( $t = -2.267$ ,  $P = 0.025$ ). In contrast to the results of radiotherapy, a higher risk score was found in patients without chemotherapy, while the patients who

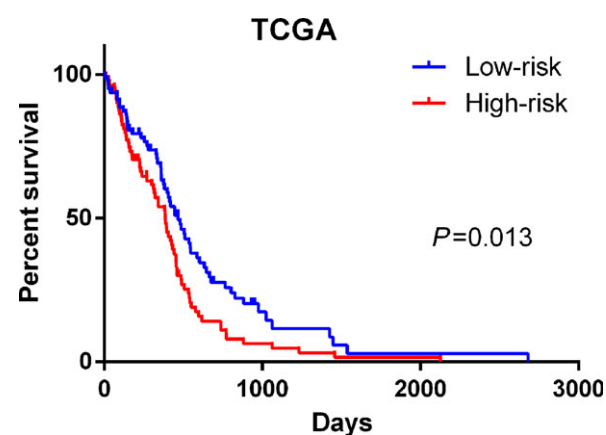


**Fig. 6.** Kaplan–Meier survival curves for the autophagy-related lncRNA risk score for glioma in TCGA dataset. Consistent with the results derived from the CGGA dataset, the high-risk patients had a shorter median OS than that of the low-risk patients in TCGA datasets (median OS 385 vs 468 days; log rank  $P = 0.012$ ).

**Table 5.** Gene set enrichment analysis results based on the signature of 10 autophagy lncRNAs.

Name	Size	ES	NES	NOM <i>P</i> -value	FDR <i>q</i> -value	FWER <i>P</i> -value	Rank	Leading edge
							at max	
Hallmark_Interferon_gamma_response	194	0.663942	2.002969	0.003831	0.03201	0.019	3784	tags = 62%, list = 18%, signal = 74%
Hallmark_Coagulation	134	0.546977	1.968419	0	0.024199	0.027	4273	tags = 47%, list = 20%, signal = 58%
Hallmark_Allograft_rejection	196	0.606039	1.934347	0.005894	0.02353	0.037	4277	tags = 59%, list = 20%, signal = 73%
Hallmark_Epithelial_mesenchymal_transition	195	0.61046	1.914759	0.01354	0.02293	0.051	4360	tags = 62%, list = 20%, signal = 77%
Hallmark_Interferon_alpha_response	95	0.695722	1.901815	0.007937	0.020948	0.057	3003	tags = 61%, list = 14%, signal = 71%
Hallmark_Il6_jak_stat3_signaling	86	0.627249	1.854703	0.011905	0.02949	0.083	4232	tags = 60%, list = 20%, signal = 75%
Hallmark_Tnfa_signaling_via_nfkb	197	0.609462	1.79719	0.024	0.041906	0.129	4243	tags = 58%, list = 20%, signal = 72%
Hallmark_Angiogenesis	35	0.582243	1.740052	0.005988	0.059463	0.178	4728	tags = 57%, list = 22%, signal = 73%
Hallmark_Complement	192	0.472855	1.732826	0.026263	0.056876	0.188	3996	tags = 45%, list = 19%, signal = 55%
Hallmark_Hypoxia	197	0.484747	1.725543	0.034068	0.053391	0.195	3666	tags = 45%, list = 17%, signal = 54%
Hallmark_Glycolysis	194	0.445341	1.707246	0.014	0.055343	0.223	4979	tags = 49%, list = 23%, signal = 64%
Hallmark_Il2_stat5_signaling	196	0.451793	1.706509	0.017341	0.050981	0.223	5329	tags = 54%, list = 25%, signal = 71%
Hallmark_Reactive_oxygen_species_pathway	46	0.522081	1.675037	0.017964	0.061012	0.263	2719	tags = 39%, list = 13%, signal = 45%
Hallmark_Inflammatory_response	194	0.527449	1.670621	0.037549	0.057958	0.266	5277	tags = 59%, list = 25%, signal = 77%
Hallmark_P53_pathway	195	0.411785	1.645334	0.027559	0.063102	0.302	4075	tags = 38%, list = 19%, signal = 47%
Hallmark_Kras_signaling_up	198	0.419712	1.634183	0.028	0.063116	0.318	4808	tags = 51%, list = 22%, signal = 64%
Hallmark_Apoptosis	159	0.432405	1.616621	0.023529	0.066577	0.339	5324	tags = 53%, list = 25%, signal = 71%
Hallmark_Apical_surface	44	0.402856	1.481723	0.034483	0.132731	0.539	1498	tags = 23%, list = 7%, signal = 24%
Hallmark_Mtorc1_signaling	193	0.417297	1.473019	0.094378	0.130749	0.55	4257	tags = 44%, list = 20%, signal = 54%
Hallmark_Apical_junction	195	0.35423	1.457525	0.066148	0.133971	0.567	3822	tags = 33%, list = 18%, signal = 40%

ES, enrichment score; FDR, false discovery rate; FWER, familywise-error rate; NES, normalized enrichment score; NOM *P* Value, nominal *P* Value.

had received chemotherapy presented a lower risk score. Moreover, we also assessed differences in risk score based on molecular status. As a result, lower risk scores were found in those with the *IDH* mutation than in those without, indicating a potential association between the lncRNA signature and *IDH* mutation.

### Validation in the TCGA dataset

Next, these results were further validated in the additional dataset (TCGA) using the same  $\beta$  value. In total, 160 GBM patients were enrolled for the validation of the lncRNA signature (Fig. 5). We divided these patients into the high-risk and low-risk groups on the basis of the median value of the risk score. Consistent with the results derived from the CGGA dataset, the high-risk patients had a shorter median OS than that of the low-risk patients (median OS 385 vs 468 days; log rank  $P = 0.012$ ; Fig. 6). This finding was further validated by Cox regression analysis, in which the high-risk group tended to have a shorter OS time for GBM patients than that of the low-risk group (HR = 1.544, 95% CI: 1.110–2.231;  $P = 0.031$ ). In light of these results, we could confirm that the

lncRNA signature provides a robust prediction for the prognosis of glioma patients.

### Gene set enrichment analysis

Further functional annotation was conducted through GSEA. The results revealed that the differentially expressed genes between the two groups were enriched in the autophagy-related and tumor-related pathways. As result, a total of 19 gene sets were significantly enriched at a nominal *P*-value < 5% (Table 5). Among the gene sets, several pathways are well-established in cancers, including interleukin (IL) 6/Janus kinase/signal transducer and activator of transcription (STAT) 3 signaling, tumor necrosis factor  $\alpha$  signaling via nuclear factor- $\kappa$ B, IL2/STAT5 signaling, the p53 pathway and the KRAS signaling pathway (Fig. 7). Moreover, the gene sets were also found to be involved in the vital functions of tumorigenesis and progression of cancer. For instance, epithelial mesenchymal transition, angiogenesis and hypoxia were closely related to the invasion and metastasis of cancer (Fig. 8). Notably, the GSEA revealed that the gene sets were involved in the reactive oxygen species pathway, interferon (IFN)- $\gamma$

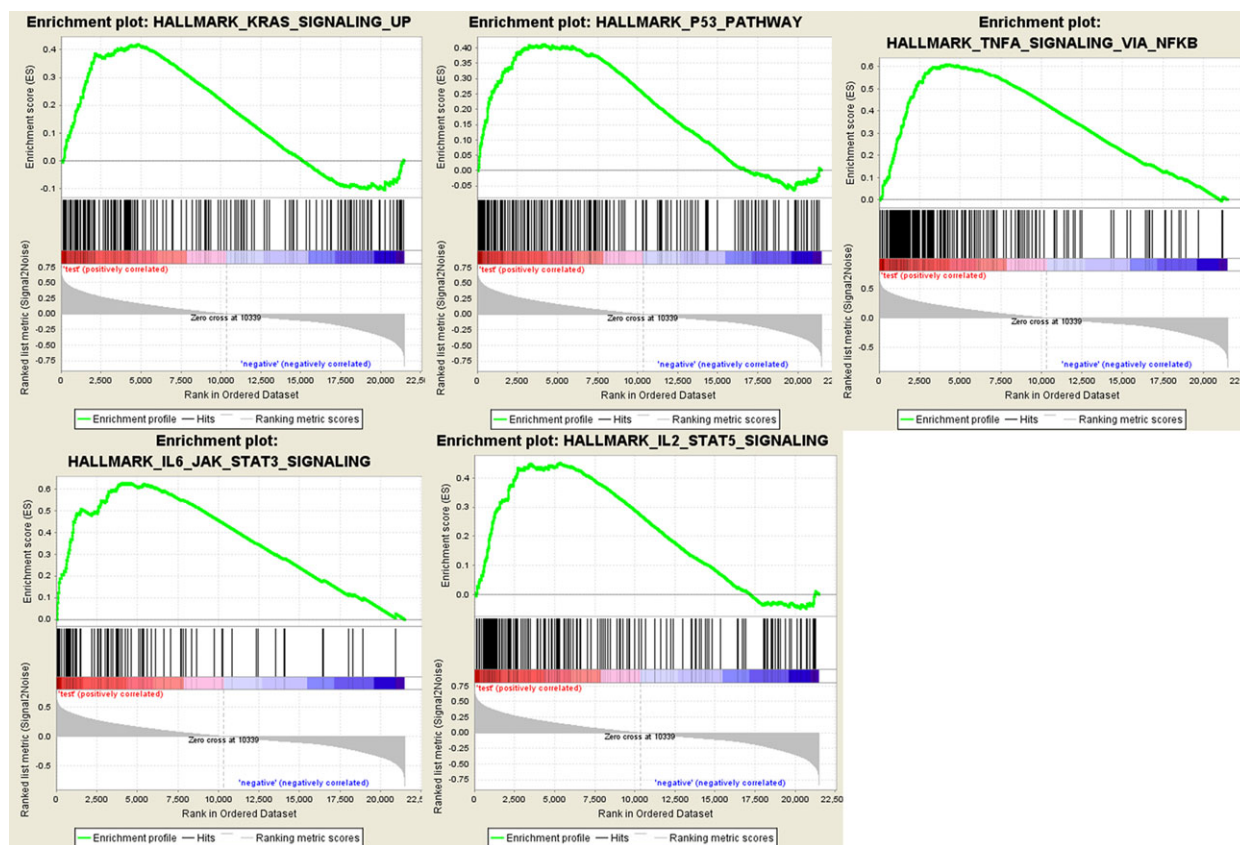


**Fig. 7.** Gene set enrichment analysis indicated significant enrichment of hallmark cancer-related pathways in the high-risk group based on CCGA dataset. JAK, Janus kinase; NFKB, nuclear factor- $\kappa$ B; TNFA, tumour necrosis factor  $\alpha$ .

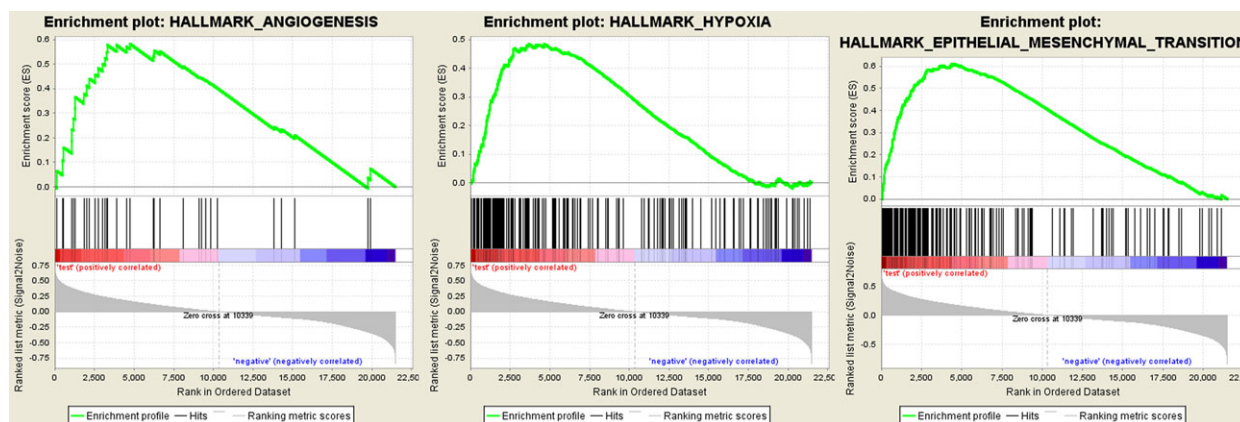


**Fig. 8.** Gene set enrichment analysis indicated significant enrichment of the progression- and metastasis-related pathway in the high-risk group based on CCGA dataset.

response, IFN- $\alpha$  response and inflammatory response, which are strongly associated with autophagy (Fig. 9). Taken together, the defined autophagy-related genes

contribute to vital cancer and autophagy pathways, which might provide strong evidence for a cancer-targeted treatment for glioma.

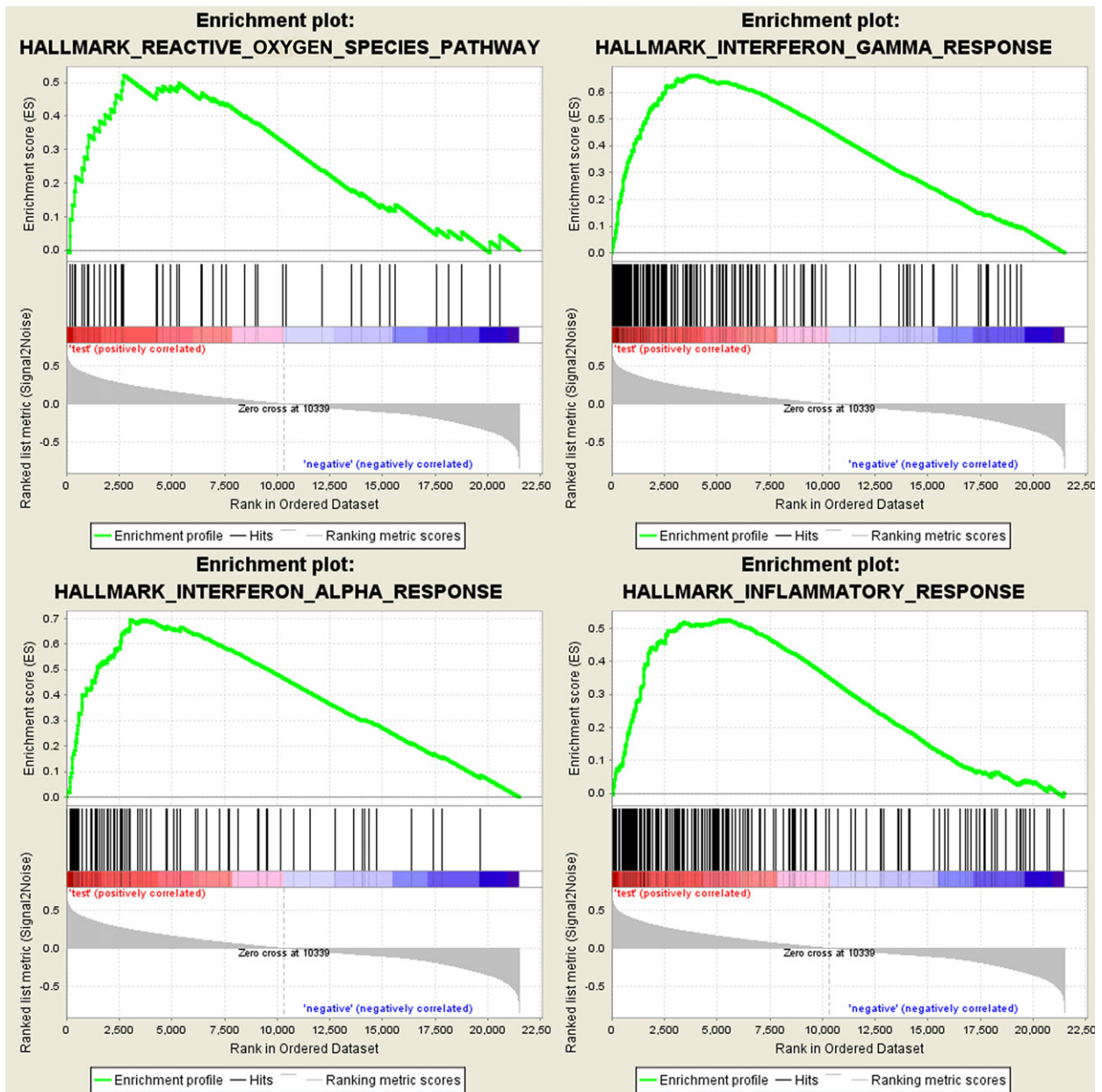


**Fig. 9.** Gene set enrichment analysis indicated significant autophagy-related enrichment based on CCGA dataset.

## Discussion

Glioma is the most aggressive and common type of primary brain tumor in humans. With the development of clinical management of glioma, some prognostic factors are well characterized, including tumor size, tumor grade and stage. High-throughput biological technologies are being widely used to predict cancer recurrence and tumor metastasis by detecting the alteration of miRNAs or genes [23,24]. The major class of

lncRNAs, as a complement to genes or miRNAs, provides a promising opportunity to predict the risk of recurrence of glioma [25]. However, so far, there has been no systematic process to identify lncRNA signature sets for predicting the survival of glioma patients. Therefore, it is necessary to establish a lncRNA signature to predict the prognosis of glioma patients.

In this study, two datasets (CGGA and TCGA) were collected to explore the prognosis of autophagy-related lncRNAs for glioma patients. In the first step,

we identified 402 lncRNAs through the lncRNA–autophagy gene co-expression network. Furthermore, we identified 10 autophagy-associated lncRNA signatures that could divide glioma patients into high- and low-risk groups based on the median risk score. Additionally, it was found that the OS is longer in the low-risk group than that in the high-risk group. Through univariate and multivariate Cox regression analyses, we can conclude that the signature is an independent factor that is significantly related to OS.

Although little is known about the role of autophagy in cancer therapy to date, recent studies suggest that autophagy therapy will become a new approach to glioma treatment [26,27]. In recent studies, IFN- $\gamma$  was found to influence autophagy and cell growth in human hepatocellular carcinoma (HCC) cells. IFN- $\gamma$  is a cytokine with anti-viral and immune regulation. The cytokine induces autophagosome formation and transformation of microtubule-associated protein 1 light chain 3 proteins and can inhibit cell growth and non-apoptotic cell death in Huh7 cells. In addition, autophagy in Huh7 cells is also activated by the overexpression of interferon-regulatory factor-1. Eventually, induced autophagy will inhibit IFN- $\gamma$  and cell death in HCC [28]. Since autophagy can respond to a variety of stresses to promote the survival of cancer cells, it has protumorigenic functions. Glucose metabolism promotes adhesion-independent conversion driven by oncogene insult-mutationally active Ras. In human cancer cell lines carrying KRAS mutations and cells ectopically expressing oncogenic H-Ras, autophagy is induced after the extracellular matrix is isolated. If autophagy is inhibited by RNA interference-mediated depletion of multiple autophagic regulators or genetic deletion, Ras-mediated conversion and glycolytic capacity proliferation independent of adhesion will be impaired. In addition, when the availability of glucose is decreased, the conversion and proliferation of autophagy-deficient cells expressing oncogenic Ras are unaffected, which is just the opposite of that in autophagy-competent cells. In conclusion, autophagy can promote the unique mechanism of Ras-driven tumor growth in specific metabolic environments [29].

Among the 10 autophagy-related lncRNAs, *PCBP1-AS1*, *DHRS4-AS1*, *MAPKAPK5-AS1* and *GABPB1-AS1* were risk-associated genes, while *TP53TGI*, *ZNF674-AS1*, *DDX11-AS1*, *SBF2-AS1*, *MIR4453HG* and *COX10-AS1* were protective genes. Specifically, we also found that the high-risk group was enriched in the glycolysis pathway. Consistent with our studies, a recent study revealed that *TP53TGI* might affect the expression of glucose metabolism-related genes under glucose deprivation, leading to cell proliferation and migration

of glioma cells [30]. Additionally, *MAPKAPK5-AS1* regulates gene expression by acting with miRNAs and is significantly associated with the OS of liver cancer [31]. Furthermore, the expression of *COX10-AS1* in oral cavity and oropharyngeal squamous cell carcinoma is more than twice that of normal cells [32].

All of the lncRNAs we identified directly or indirectly regulate autophagy, many by regulating miRNAs; thus, we must perform lncRNA–mRNA co-expression analyses to assess the function of lncRNAs [33–35]. Therefore, we can conclude that due to the various functions of lncRNAs, the 10 autophagy-related lncRNAs we identified will be potential therapeutic targets [12,36].

In conclusion, by constructing an autophagy–lncRNA coexpression network, we identified a signature of 10 autophagy-related lncRNAs, which has prognostic value for glioma patients. In addition, our study classified low-risk and high-risk groups based on the median risk score, and each showed different autophagy states.

## Acknowledgements

This work was supported by Guangxi Medical Health Appropriate Technology Development and Application Project (S2017099).

## Conflict of interest

The authors declare no conflict of interest.

## Author contributions

LM designed the study, and revised the manuscript. FL, the main author of study, conceived and designed the analysis and wrote the manuscript. WC and MC took part in analyzing the data and writing the manuscript. JY and HC analyzed the data and conducted the results. HY and TL contributed to writing and revising the manuscript. All authors read and approved the final manuscript.

## References

- 1 Reni M, Mazza E, Zanon S, Gatta G and Vecht CJ (2017) Central nervous system gliomas. *Crit Rev Oncol Hematol* **113**, 213–234.
- 2 Louis DN, Ohgaki H, Wiestler OD, Cavenee WK, Burger PC, Jouvet A, Scheithauer BW and Kleihues P (2007) The 2007 WHO classification of tumours of the central nervous system. *Acta Neuropathol* **114**, 97–109.
- 3 Shergalis A, Bankhead A, Luesakul U, Muangsin N and Neamati N (2018) Current challenges and

- opportunities in treating glioblastoma. *Pharmacol Rev* **70**, 412–445.
- 4 Ohgaki H, Dessen P, Jourde B, Horstmann S, Nishikawa T, Di Patre P-L, Burkhard C, Schüler D, Probst-Hensch NM and Maiorka PC (2004) Genetic pathways to glioblastoma: a population-based study. *Can Res* **64**, 6892–6899.
  - 5 Maher EA, Brennan C, Wen PY, Durso L, Ligon KL, Richardson A, Khatry D, Feng B, Sinha R and Louis DN (2006) Marked genomic differences characterize primary and secondary glioblastoma subtypes and identify two distinct molecular and clinical secondary glioblastoma entities. *Can Res* **66**, 11502–11513.
  - 6 Parsons DW, Jones S, Zhang X, Lin JC-H, Leary RJ, Angenendt P, Mankoo P, Carter H, Siu I-M and Gallia GL (2008) An integrated genomic analysis of human glioblastoma multiforme. *Science* **321**, 1807–1812.
  - 7 Levine B and Kroemer G (2008) Autophagy in the pathogenesis of disease. *Cell* **132**, 27–42.
  - 8 Janku F, McConkey DJ, Hong DS and Kurzrock R (2011) Autophagy as a target for anticancer therapy. *Nat Rev Clin Oncol* **8**, 528.
  - 9 Amaravadi RK, Lippincott-Schwartz J, Yin X-M, Weiss WA, Takebe N, Timmer W, DiPaola RS, Lotze MT and White E (2011) Principles and current strategies for targeting autophagy for cancer treatment. *Clin Cancer Res* **17**, 654–666.
  - 10 Sui X, Chen R, Wang Z, Huang Z, Kong N, Zhang M, Han W, Lou F, Yang J and Zhang Q (2013) Autophagy and chemotherapy resistance: a promising therapeutic target for cancer treatment. *Cell Death Dis* **4**, e838.
  - 11 Lefranc F, Facchini V and Kiss R (2007) Proautophagic drugs: a novel means to combat apoptosis-resistant cancers, with a special emphasis on glioblastomas. *Oncologist* **12**, 1395–1403.
  - 12 Mercer TR, Dinger ME and Mattick JS (2009) Long non-coding RNAs: insights into functions. *Nat Rev Genet* **10**, 155.
  - 13 Chen YG, Satpathy AT and Chang HY (2017) Gene regulation in the immune system by long noncoding RNAs. *Nat Immunol* **18**, 962.
  - 14 Bian EB, Li J, Xie YS, Zong G, Li J and Zhao B (2015) LncRNAs: new players in gliomas, with special emphasis on the interaction of lncRNAs With EZH2. *J Cell Physiol* **230**, 496–503.
  - 15 Yao Y, Li J and Wang L (2014) Large intervening non-coding RNA HOTAIR is an indicator of poor prognosis and a therapeutic target in human cancers. *Int J Mol Sci* **15**, 18985–18999.
  - 16 Chondrogianni N, Petropoulos I, Grimm S, Georgila K, Catalgol B, Friguet B, Grune T and Gonos ES (2014) Protein damage, repair and proteolysis. *Mol Aspects Med* **35**, 1–71.
  - 17 O'Dwyer DN, Ashley SL and Moore BB (2016) Influences of innate immunity, autophagy, and fibroblast activation in the pathogenesis of lung fibrosis. *Am J Physiol Lung Cell Mol Physiol* **311**, L590–L601.
  - 18 Bhan A and Mandal SS (2015) LncRNA HOTAIR: a master regulator of chromatin dynamics and cancer. *Biochim Biophys Acta* **1856**, 151–164.
  - 19 Yang L, Zhang X, Li H and Liu J (2016) The long noncoding RNA HOTAIR activates autophagy by upregulating ATG3 and ATG7 in hepatocellular carcinoma. *Mol BioSyst* **12**, 2605–2612.
  - 20 Ge D, Han L, Huang S, Peng N, Wang P, Jiang Z, Zhao J, Su L, Zhang S and Zhang Y (2014) Identification of a novel MTOR activator and discovery of a competing endogenous RNA regulating autophagy in vascular endothelial cells. *Autophagy* **10**, 957–971.
  - 21 Sun T (2017) Long noncoding RNAs act as regulators of autophagy in cancer. *Pharmacol Res* **129**, 151–155.
  - 22 Shannon P, Markiel A, Ozier O, Baliga NS, Wang JT, Ramage D, Amin N, Schwikowski B and Ideker T (2003) Cytoscape: a software environment for integrated models of biomolecular interaction networks. *Genome Res* **13**, 2498–2504.
  - 23 van't Veer LJ, Rutgers EJ and Piccart M (2016) 70-Gene signature in early-stage breast cancer. *N Engl J Med* **375**, 2200.
  - 24 Lerebours F, Cizeron-Clairac G, Susini A, Vacher S, Mouret-Fourme E, Belichard C, Brain E, Alberini JL, Spyrtos F and Lidereau R (2013) miRNA expression profiling of inflammatory breast cancer identifies a 5-miRNA signature predictive of breast tumor aggressiveness. *Int J Cancer* **133**, 1614–1623.
  - 25 Niknafs YS, Han S, Ma T, Speers C, Zhang C, Wilder-Romans K, Iyer MK, Pitchiaya S, Malik R and Hosono Y (2016) The lncRNA landscape of breast cancer reveals a role for DSCAM-AS1 in breast cancer progression. *Nat Commun* **7**, 12791.
  - 26 Takeuchi H, Kondo Y, Fujiwara K, Kanzawa T, Aoki H, Mills GB and Kondo S (2005) Synergistic augmentation of rapamycin-induced autophagy in malignant glioma cells by phosphatidylinositol 3-kinase/protein kinase B inhibitors. *Can Res* **65**, 3336–3346.
  - 27 Pavlides S, Vera I, Gandara R, Sneddon S, Pestell RG, Mercier I, Martinez-Outschoorn UE, Whitaker-Menezes D, Howell A and Sotgia F (2012) Warburg meets autophagy: cancer-associated fibroblasts accelerate tumor growth and metastasis via oxidative stress, mitophagy, and aerobic glycolysis. *Antioxid Redox Signal* **16**, 1264–1284.
  - 28 Li P, Du Q, Cao Z, Guo Z, Evankovich J, Yan W, Chang Y, Shao L, Stolz DB and Tsung A (2012) Interferon-gamma induces autophagy with growth inhibition and cell death in human hepatocellular carcinoma (HCC) cells through interferon-regulatory factor-1 (IRF-1). *Cancer Lett* **314**, 213–222.

- 29 Lock R, Roy S, Kenific CM, Su JS, Salas E, Ronen SM and Debnath J (2011) Autophagy facilitates glycolysis during Ras-mediated oncogenic transformation. *Mol Biol Cell* **22**, 165–178.
- 30 Chen X, Gao Y, Li D, Cao Y and Hao B (2017) LncRNA-TP53TG1 participated in the stress response under glucose deprivation in glioma. *J Cell Biochem* **118**, 4897–4904.
- 31 Zhang J, Fan D, Jian Z, Chen GG and Lai PB (2015) Cancer specific long noncoding RNAs show differential expression patterns and competing endogenous RNA potential in hepatocellular carcinoma. *PLoS One* **10**, e0141042.
- 32 Feng L, Houck JR, Lohavanichbutr P and Chen C (2017) Transcriptome analysis reveals differentially expressed lncRNAs between oral squamous cell carcinoma and healthy oral mucosa. *Oncotarget* **8**, 31521.
- 33 Guo Q, Cheng Y, Liang T, He Y, Ren C, Sun L and Zhang G (2015) Comprehensive analysis of lncRNA-mRNA co-expression patterns identifies immune-associated lncRNA biomarkers in ovarian cancer malignant progression. *Sci Rep* **5**, 17683.
- 34 Liu Z, Li X, Sun N, Xu Y, Meng Y, Yang C, Wang Y and Zhang K (2014) Microarray profiling and co-expression network analysis of circulating lncRNAs and mRNAs associated with major depressive disorder. *PLoS One* **9**, e93388.
- 35 Li H, Wang W, Zhang L, Lan Q, Wang J, Cao Y and Zhao J (2017) Identification of a long noncoding RNA-associated competing endogenous RNA network in intracranial aneurysm. *World Neurosurg* **97**, 684–692.e4.
- 36 Fang Y and Fullwood MJ (2016) Roles, functions, and mechanisms of long non-coding RNAs in cancer. *Genomics Proteomics Bioinformatics* **14**, 42–54.